

1 **Local impact analysis of climate change on precipitation** 2 **extremes: are high-resolution climate models needed for** 3 **realistic simulations?**

4 Hossein Tabari¹, Rozemien De Troch^{2,5}, Olivier Giot^{2,6}, Rafiq Hamdi^{2,5}, Piet Termonia^{2,5}, Sajjad Saeed³,
5 Erwan Brisson³, Nicole Van Lipzig³ and Patrick Willems^{1,4}

6 ¹Hydraulics Division, Department of Civil Engineering, KU Leuven, Kasteelpark Arenberg 40, BE-3001 Leuven,
7 Belgium.

8 ²Royal Meteorological Institute of Belgium, Brussels, Belgium.

9 ³Department of Earth and Environmental Sciences, KU Leuven, Leuven, Belgium.

10 ⁴Department of Hydrology and Hydraulic Engineering, Vrije Universiteit Brussel, Belgium.

11 ⁵Department of Physics and Astronomy, Ghent University, Belgium.

12 ⁶Plant and Vegetation Ecology, University of Antwerp, Belgium.

13 *Correspondence to:* Hossein Tabari (hossein.tabari@kuleuven.be; tabari.ho@gmail.com)

14 **Abstract.** This study explores whether climate models with higher spatial resolution provide higher accuracy for
15 precipitation simulations and/or different climate change signals. The outputs from two convection-permitting
16 climate models (ALARO and CCLM) with a spatial resolution of 3-4 km are compared with those from the coarse
17 scale driving models or reanalysis data for simulating/projecting daily and sub-daily precipitation quantiles.
18 Validation of historical design precipitation statistics derived from intensity–duration–frequency (IDF) curves shows
19 a better match of the convection-permitting model results with the observations-based IDF statistics compared to the
20 driving GCMs and reanalysis data. This is the case for simulation of local sub-daily precipitation extremes during
21 the summer season, while the convection-permitting models do not appear to bring added value to simulation of
22 daily precipitation extremes. Results moreover indicate that one has to be careful in assuming spatial scale
23 independency of climate change signals for the delta change downscaling method, as high-resolution models may
24 show larger changes in extreme precipitation. These larger changes appear to be dependent on the time scale, since
25 such intensification is not observed for daily time scale for both the ALARO and CCLM models.

26 **1 Introduction**

27 It becomes evident that climate change will increase the frequency and intensity of extreme events (IPCC, 2007,
28 2013). Therefore, the impacts of climate change on hydrological extremes such as heavy precipitation events have to
29 be considered when designing and optimizing water infrastructures. The future projection of climate change impact
30 on precipitation usually relies on the simulation results of General Circulation Models (GCMs). However, these
31 results need to be validated against historical precipitation observations prior to any use for local impact studies of
32 climate change. When GCM results are validated based on observations, sometimes large biases are observed
33 especially for extreme precipitation values (van Pelt et al., 2012; van Haren et al., 2013; Tabari et al., 2015),
34 imposing an uncertainty to the GCM projections for the future. The biases in the coarse-resolution GCMs come

1 from the fact that they disregard some governing features of precipitation at local scale, next to the scale differences
2 when comparing GCM results with local observations (Maraun et al., 2010; Willems et al., 2012). Some previous
3 studies that attempted to assess GCM skill as a function of resolution showed that the performance of GCMs is
4 independent of their resolution (Johnson et al., 2011; Masson and Knutti, 2011). However, given that deep
5 convective phenomena are sufficiently resolved only at spatial resolutions up to less than about 4 km, such
6 dynamical downscaling is expected to be one of the solutions for decreasing the systematic biases and narrowing the
7 gap between GCM outputs and needs for fine-scale precipitation in hydrological and water engineering studies.

8 One of the methods to dynamically downscale GCM outputs is to drive a Regional Climate Model (RCM) using
9 GCM as initial and boundary conditions. RCMs usually provide an improved description of surface features
10 (topographical, land cover, etc.) and more complex description of atmospheric processes compared to GCMs. This
11 often results in more realistic representation of precipitation variability and of climate feedback mechanisms (IPCC,
12 2001; Mearns et al., 2004; Christensen and Christensen, 2007; Mayer et al., 2015). Whatever climate models are
13 used, verification of their results under the current climate is needed, because some high-resolution RCMs fail to
14 adequately describe local-scale surface processes (especially in inhomogeneous regions with complex topography)
15 due to the convective parameterization scheme or the characteristics of the GCM they are nested in (Hohenegger et
16 al., 2008; Willems et al., 2012).

17 High-resolution (convection-permitting resolutions) climate models are of great added value to simulate large
18 convective storms and mesoscale organization (Kendon et al., 2014; Prein et al., 2015). At these resolutions, deep
19 convection is partly resolved and does not need to rely entirely on parameterizations. The representation of the daily
20 cycle in precipitation, extreme events and spatial variability strongly improves for convection-permitting models
21 (Kendon et al., 2012; Prein et al., 2013a, 2013b, 2015; Brisson et al., 2015; Ban et al., 2014, 2015, Fosser et al.,
22 2015, 2016). However, their long-term simulation is restricted due to high computational costs. They are
23 consequently mainly applied for numerical weather prediction (Done et al., 2004; Baldauf et al., 2011; Tang et al.,
24 2013). First simulations for decadal time periods using convection-permitting models point to a stronger increase in
25 extremes compared to coarser resolution integration, but the number of climate change impact studies with these
26 models is limited so far (Hohenegger et al., 2008; Kendon et al., 2012, 2014; Prein et al., 2015).

27 The use of regional climate models for local impact studies of climate change on precipitation (totals or
28 extremes) has been increased in recent years (e.g. Willems and Vrac, 2011; Olsson et al., 2012; Mearns et al., 2013;
29 Rajczak et al., 2013; Olsson et al., 2015). Nevertheless, in some studies, climate scenarios have been based on a
30 broad set of coarse-resolution GCM results (Deng et al., 2013; Rana et al., 2014; Sun et al., 2015). Now, the
31 question is whether high-resolution climate models truly improve extreme precipitation simulations, and if so, to
32 what extent. This study intends to answer this research question by comparing high-resolution models (RCMs with
33 resolutions between 40 and 3 km) with their driving GCM or reanalysis data for simulating sub-daily and daily
34 precipitation quantiles. Further comparisons are performed for simulating design precipitation statistics derived from
35 intensity–duration–frequency (IDF) curves.

36 Second research question considered, in case the high resolution climate models show improved extreme
37 precipitation results, is whether this improvement in absolute precipitation values also significantly changes the

1 relative climate change signal. Hydrological applications of climate change impact analysis often assume that the
2 precipitation change factors, defined as the relative change from historical to future climate conditions, can be
3 obtained from GCM or RCM simulations and applied for impact analysis at finer spatial scales. This is the case for
4 any delta change or perturbation based statistical downscaling method (e.g. Ntegeka et al., 2014; Sunyer et al.,
5 2015). In this study, the validity of this hypothesis is investigated by comparing the climate change signals between
6 the high and coarse scale resolution models. Central Belgium is considered as the study location.

7 **2 Climate models**

8 **2.1 ALARO model**

9 The ALARO-0 model is a high-resolution regional climate model developed by the Royal Meteorological Institute
10 (RMI) of Belgium based on the numerical weather prediction model called Aire Limitee Adaptation Dynamique
11 Developpement International (ALADIN). Hereafter, ALARO is used as shorthand name for the ALARO-0 model
12 described in De Troch et al. (2013). The ALADIN model is the limited area model (LAM) version of the Action de
13 Recherche Petite Echelle Grande Echelle Integrated Forecast System (ARPEGE-IFS). The physics parameterization
14 package of the ALARO model was designed specifically for running at resolutions between 3 and 8 km. The
15 specific characteristics of the Modular Multiscale Microphysics and Transport (3MT) convection scheme used in the
16 ALARO model lead to a good multiscale performance, particularly in convection-permitting resolutions (De Troch
17 et al., 2013). The ALARO simulations for the present climate conditions over Belgium were performed for the
18 periods 1961-1990 and 1981-2010 at resolutions ranging from 40 km down to 4 km, both using a set of simulations
19 forced with ERA-40 or ERA-Interim reanalysis as well as with the CNRM-CM3 GCM for the historical control run
20 (Table 1). For the future climate projections (2071–2100), the CNRM-CM3 GCM under the A1B scenario was used
21 to force the ALARO model (Hamdi et al., 2014).

22 **2.2 CCLM model**

23 The other high-resolution climate model used in this study is the COSMO-CLM (CCLM) model. The CCLM is a
24 non-hydrostatic limited area climate model developed by the climate limited-area modeling (CLM) community. The
25 CCLM model is based on the COSMO model (Steppeler et al., 2003), designed by the Deutsche Wetterdienst
26 (DWD) for operational weather prediction. In order to perform climate simulations with the COSMO model, the
27 CLM community provided extensions such as dynamic surface boundaries, a more complex soil model and the
28 possibility to use various CO₂ concentration values (Böhm et al., 2006; Rockel et al., 2008).

29 The model settings are based on a previous study by Brisson et al. (2015), which provide recommendations for
30 performing climate simulations at convection permitting scale. The one-moment microphysical parameterization
31 includes a representation of graupel hydrometeors. In addition, the domain size of this simulation (192x175
32 gridpoints) is large enough to ensure that the analysis is not affected by the spatial spin-up described in Brisson et al.
33 (2015). The integration scale of global models largely differs from convection permitting scale. A multiple nesting
34 strategy was therefore selected to carry out such simulations (Brisson et al. 2015, 2016). A three-step nesting

1 strategy was applied with the driving data, either from ERA-Interim reanalysis data or the EC-EARTH GCM,
2 forcing a CCLM at 25 km grid mesh size, which in turn forces a CCLM at 7 km grid mesh size, and next at the final
3 2.8 km grid mesh size. Model simulations were performed for the period 2001-2010, and a thorough evaluation of
4 the statistics of precipitation, temperature and cloud characteristics was recently performed (Brisson et al., 2016).
5 The CCLM driven by EC-EARTH was performed for the period 2000-2010 and 2060-2069 using the RCP4.5
6 emission scenario (Table 1). Hereafter, the driving GCM or reanalysis dataset is shown as subscript to the name of
7 the RCM. As the control run of the EC-EARTH GCM ends in 2009, its data for the period 2000-2009 were used for
8 comparing with the driven CCLM simulations.

9 **3 Methodology**

10 In this study, simulations of sub-daily and daily precipitation quantiles from the climate models are analyzed. For
11 the future climate analysis, the climate change signals are obtained as relative changes of precipitation intensities
12 calculated as the ratios of precipitation quantiles derived from each climate model scenario simulation over those
13 from the corresponding climate model control simulation with same non-exceedance probability or return period.
14 This methodology has been applied in several recent climate change studies, e.g. on the basis of statistical
15 downscaling applying quantile mapping or quantile perturbations (Willems and Vrac, 2011; Gudmundsson et al.,
16 2012; Maraun, 2013; Ntegeka et al., 2014; Rana et al., 2014; Sunyer et al., 2015) and also a similar procedure for
17 analyzing decadal precipitation anomaly (Tabari et al., 2014; Tabari and Willems, 2016). For sub-daily precipitation,
18 independent extremes are selected using a Peak Over Threshold (POT) method. The POT selection is done based on
19 three criteria for inter-event time, inter-event low precipitation and peak height, similar to those presented by
20 Willems (2009) for extracting POT values for discharge. The inter-event time is the main criterion for extraction of
21 POT values. Following Willems (2013), an inter-event time of 12 hours is selected, implying that two successive
22 precipitation peaks within the same day or night are considered as one extreme event. In other words, two
23 consecutive precipitation extremes are interpreted to be independent based on this criterion when the time between
24 the two events exceeds 12 hours. Extreme precipitation is defined in this study as precipitation with return period (T)
25 higher than 1 year. The return period is in this study calculated in two different ways: empirically based on the rank
26 of the extracted POT values (n/i , where n and i are the length of the study period and rank, respectively; $i = 1$ for the
27 highest value); and theoretically after calibrating an extreme value distribution to these POT precipitation extremes.
28 Also for the calculation of the precipitation change factors for given return periods, these two different approaches
29 were followed and compared: empirical data based and extreme value distribution based change factors. For the
30 distribution based change factors, first a distribution is fitted separately to the extreme values of the control and
31 scenario runs of the climate models. Afterwards, change factors are computed as a ratio between the fitted
32 distribution values of the scenario and control runs.

33 In addition to the quantile analysis, the historical simulations of the climate models are validated based on
34 precipitation intensity–duration–frequency (IDF) curves which are typically used for design storm calculations and
35 related designs, e.g., urban drainage systems and hydraulic structures. The IDF curves for 1-month, 1-year and 10-
36 year return periods and for durations from 10-15 minutes up to one month are developed for the control runs of the

1 climate models as well as the observations. The IDF curves are derived based on POT extreme value statistics after
2 calibration of two-component exponential distributions, following Willems (2000). In this paper, the precipitation
3 intensities of given return periods are referred to as design precipitation quantiles.

4 For the climate models, precipitation data are extracted from a matrix of 3×3 model grid points (9 cells)
5 surrounding the closest model grid point to Uccle station in Central Belgium. This station is selected because it has
6 high quality 10-min observations recorded with same instrument since 1898 (Demarée, 2003). In addition to the 10-
7 min station observations, daily E-OBS gridded data (v12.0, Haylock et al., 2008) for 27.8 km and 55.7 km are used.
8 These gridded data are aggregated to larger pixels of 167 km and 334 km to be consistent with the grid mesh size of
9 the driving GCMs and reanalysis data. The aggregation is also performed to upscale the outputs of the convection-
10 permitting climate models to check the accuracy of the spatial structure in the models.

11 **4 Validation of precipitation simulations**

12 The capability of the climate models to simulate the present-day precipitation is evaluated before investigating
13 future precipitation changes. Prior to this performance evaluation, the precipitation extremes from the model grid
14 cell covering Uccle station are compared with those from neighboring cells for possible outlier or unrealistic values.
15 The analysis shows spatial consistency in the frequency of daily and sub-daily precipitation extremes for both the
16 ALARO and CCLM models. As an example, Fig. 1 illustrates hourly precipitation extremes in a matrix of 3×3
17 ALARO_{ERA-Interim} 4 km model grid points surrounding the closest model grid point to Uccle station for summer and
18 winter seasons. It is seen that hourly precipitation extremes in gridcell 5 covering Uccle station are consistent with
19 the ones in the neighboring gridcells. Another preliminary analysis is performed to compare point and pixel
20 interpolated Uccle precipitation observations, which are used as reference for the model performance evaluation
21 (Fig. 2). The comparison is done for the periods 1961-1990 and 2001-2010, which are the control periods of the
22 ALARO and CCLM models, respectively. The precipitation extremes from the pixel E-OBS data follow the pattern
23 of the point observations and the extremes are well represented in the pixel dataset. The smaller amounts from the
24 gridded dataset is due to the fact that spatial averaging smooths out the extreme values (Hofstra et al., 2010; Sunyer
25 et al., 2013).

26 The validation results of the daily precipitation quantiles simulated by the ALARO convection-permitting
27 models and its boundary conditions based on the point and pixel interpolated Uccle observations for the summer
28 season (June-July-August: JJA) are shown in Fig. 3. The precipitation extremes for each model run are evaluated on
29 the native model grids, and are then aggregated to a larger model grid size in order to ensure a fair comparison. For
30 the aggregation purpose, the coarsest grid is used as reference. It means that, for instance for the ALARO model, the
31 evaluation of the model with 4 and 10 km resolutions is carried out on the coarser 40 km grid. The results on the
32 native model grids are presented to evaluate whether the available climate model runs are of direct use for climate
33 change impact analysis in urban hydrology. The native daily precipitation extremes reveal the largest extreme values
34 for the ALARO_{ERA40} 4 km model (Fig. 3a). However, this might be due to the precipitation decrease after the spatial
35 averaging. The overestimation of the ALARO runs nested in the ERA40 reanalysis data is also evident on the native
36 model grids, while the extreme simulations of the ALARO_{CNRM-CM3} model with 4 km resolution are in between the

1 point observations and the gridded ones with a grid size of 27.8 km, which shows good accuracy of these
2 simulations. When comparing the model results at the same grid size (Fig. 3b), the ALARO_{ERA40} 40 km outputs are
3 larger than those from the ALARO_{ERA40} model for the higher resolutions at 4 and 10 km. This indicates the role of
4 spatial scale in the climate modeling by the ALARO model driven by the ERA40 reanalysis data. Also other authors
5 reported no improvements in the simulations of daily mean precipitation by the convection-permitting models
6 compared with large scale climate models (Chan et al., 2013; Fosser et al., 2015). Some other researchers found
7 improvements especially over mountainous areas (Prein et al., 2013b; Ban et al., 2014), implying region and model
8 dependency for simulation of daily mean precipitation. In our study, the higher skill of the ALARO_{CNRM-CM3} model
9 in simulation of summer precipitation extremes appears to be because of a better representation of the small-scale
10 characteristics and spatial variability relevant for convection (Fig. 3b). The CNRM-CM3 GCM and ERA40
11 reanalysis data used as the boundary conditions of the ALARO model show a systematic underestimation especially
12 for the higher return periods (Fig. 3a). The convection parameterization has been found to be responsible for this
13 underestimation (Kendon et al., 2014).

14 As for the CCLM model, the native daily precipitation quantiles from the 2.8 km runs are larger for most of the
15 cases (Fig. 4a). After upscaling of the finer resolution models (2.8 and 7 km) to the larger scale (25 km), the results
16 of the models become similar (Fig. 4b). The driving EC-EARTH GCM and ERA-Interim reanalysis underestimate
17 the summer extremes, probably due to the misrepresentation of the convective processes. When the results of the
18 driven GCM and reanalysis data are compared with the ones of the CCLM, the larger and more accurate simulations
19 of the CCLM model is observed for summer when convection becomes dominant. This confirms the finding that
20 higher resolution results in more extreme precipitation in climate models (Jacob et al., 2014). The increasing skill of
21 RCMs with increasing model resolution for simulation of the spatio-temporal characteristics of summer precipitation
22 has been found by using the high-resolution models, although limited in application (Rauscher et al., 2010; Kendon
23 et al., 2012). Nevertheless, a comparison between the CCLM outputs of different resolutions does not show a clear
24 difference, neither in precipitation intensity or in simulation skill (Fig. 4b).

25 The extreme precipitation (averaged over the extreme events with $T > 1$ year) simulations of the climate models
26 versus spatial scale for both summer and winter seasons are shown in Fig. 5. Taking the spatial scale difference into
27 account and averaging the extreme values with $T > 1$ year, the ALARO_{ERA40} simulations are closer to the
28 observations compared with the ALARO_{CNRM-CM3} model. Decrease in systematic biases in the large scale climate in
29 reanalysis-driven RCM simulations was also reported by Maraun et al. (2010). They also pointed out that these
30 RCMs are capable of reproducing the actual day-to-day sequence of weather events. The good accuracy of the
31 CCLM model, large underestimations of CNRM-CM3 and EC-EARTH, slight overestimation of ERA-Interim data
32 and slight underestimation of ERA40 data for summer precipitation extremes are also obvious from these plots. As
33 expected, the percentage bias of the climate models (not shown) decreases as the time scales get larger (i.e., weekly
34 and monthly).

35 The validation of the climate model simulations for the summer season in terms of IDF statistics is shown in Fig.
36 6 for time scales in the range between 10-15 minutes and 30 days. The IDF curves are plotted with reference to
37 design precipitation intensities from the station and E-OBS pixel data over the Uccle location (Central Belgium).

1 Comparing the hourly simulations of the ALARO_{ERA40} model with different resolutions shows the greater intensities
2 for finer resolutions. In terms of accuracy, all of the ALARO runs except the ALARO_{CNRM-CM3} for 10-year return
3 period and the ALARO_{ERA40} 40 km for both return periods underestimate the station observations and overestimate
4 the gridded observations (extrapolated for sub-daily precipitation based on extreme value distribution). Regarding 3-
5 and 6-hourly time scales, the ALARO model simulates more intense precipitation of 10-year return period in
6 comparison to both the station and gridded observations. The model underestimates (overestimates) extreme
7 precipitation of 1-year return period and 3- and 6-hourly durations when compared with the station (gridded)
8 observations. Daily precipitation intensity of 10-year return period derived from the point observations is
9 underestimated by the ALARO_{ERA40} and ALARO_{ERA-Interim} runs and overestimated by the ALARO_{CNRM-CM3} run,
10 while all the runs overestimate the pixel observations-based statistics. All the ALARO runs except the ALARO<sub>ERA-
11 Interim</sub> simulate larger daily precipitation extremes of 1-year return period. A comparison between the ALARO 4 km
12 runs nested in reanalysis data for larger time scales between 5 and 30 days shows overestimation of the
13 ALARO_{ERA40} and underestimation of the ALARO_{ERA-Interim} with respect to the station data, whereas both of them
14 overestimate the pixel observations-based statistics. The other ALARO 4 km run (ALARO_{CNRM-CM3}) underestimates
15 both the point and pixel observations-based statistics for these larger aggregation levels (5, 10, 15 and 30 days).

16 The CCLM model simulates less intense 15-min precipitation of 10-year return period (Fig. 6). However, this
17 underestimation changes to overestimation for larger sub-daily aggregation levels. For the sub-daily design storms
18 of 1-year return period, the CCLM model generally underestimates the station observations, while both over- and
19 underestimations are seen in comparison with the gridded observations. However, the EC-EARTH GCM extremely
20 underestimates both the gridded and raingauge observations for the 10-year return period. This supports the recent
21 findings for underestimation of heavy hourly precipitation during summer by large scale climate models and more
22 accurate simulations of convection-permitting models (Chan et al., 2013, 2014; Ban et al., 2014; Fosser et al., 2015).
23 In the case of daily duration, which are less important for urban drainage applications, the CCLM runs
24 underestimate (overestimate) precipitation intensity of 1-year return period in comparison with the point (gridded)
25 observations (Fig. 6). The underestimation of higher intensities by the CCLM 2.8 km run for summer has also been
26 reported in the literature (Fosser, 2014). For the daily precipitation extremes of 10-year return period, the 2.8 km
27 runs and the CCLM_{EC-EARTH} 25 km underestimate (overestimate) precipitation intensity from the point (gridded)
28 observations, while the rest of the CCLM runs show the opposite behavior. For the larger aggregation levels
29 between 5 and 30 days, the precipitation intensities of 1-year return period derived from both the point and pixel
30 observations are underestimated by all the CCLM runs. For the 5-day duration and 10-year return period,
31 underestimation of the station observations-based statistics and overestimation of the pixel observations-based
32 statistics are seen for all the CCLM runs except for the 7 km runs. The CCLM_{ERA-Interim} 2.8 and 7 km runs simulate
33 larger precipitation extremes for the 10-, 15- and 30-day durations of 10-year return period, whereas the CCLM<sub>ERA-
34 Interim</sub> 25 km run simulates smaller extremes. The similarity between the CCLM 2.8 and 7 km runs is expected to be
35 explained by the similarity in lateral boundary conditions since the CCLM 2.8 km model is nested in the CCLM 7
36 km model. However, the difference between these runs becomes obvious when the convection is dominant in sub-
37 daily summer precipitation as they treat deep convection in different ways. The CCLM_{EC-EARTH} 25 km run shows the

1 same pattern as the CCLM_{ERA-Interim} run: underestimation of extreme precipitation intensity for the 10-, 15- and 30-
2 day durations of 10-year return period. Both over- and underestimations are seen for the CCLM_{EC-EARTH} 2.8 and 7
3 km runs for the 10-, 15- and 30-day durations of 10-year return period (Fig. 6).

4 For the winter season (December-January-February: DJF), the results show overestimations of the ALARO and
5 CCLM models (Fig. 5). As winter precipitation over Belgium is mainly controlled by large scale circulation, an
6 improvement in the simulations of convection-permitting models in comparison to the parent large scale models is
7 less expected for the winter season. Although improved simulations of winter precipitation by convection-permitting
8 model have been reported for regions with complex topography (Ikeda et al., 2010; Rasmussen et al., 2011) due to
9 better resolved orography (Prein et al., 2015), this effect is less relevant for Belgium which is more flat. Whereas
10 winter daily precipitation extremes are systematically overestimated by the ALARO model, the driving CNRM-
11 CM3 GCM slightly underestimates the winter extremes (Fig. 5). Deficiency of very high resolution climate models
12 in simulation of winter precipitation extremes is because the fronts and synoptic depressions that cause the
13 dynamical processes driving winter precipitation events have scales of 10^2 - 10^3 km. This deficiency has been
14 demonstrated by Hong and Leetmaa (1999) and Chan et al. (2013). For the CCLM model, when the CCLM_{EC-EARTH}
15 2.8 and 7 km simulations are compared with those of the CCLM_{ERA-Interim} 2.8 and 7 km for the daily winter extremes,
16 the overestimations of the earlier runs are higher than the later ones, while for larger time scales (weekly and
17 monthly) the opposite pattern is observed.

18 **5 Future precipitation changes**

19 To cope with the scale difference and the biases shown in the previous section, state-of-the-art climate change
20 impact analysis makes use of statistical downscaling. One of the popular downscaling methods is the delta change
21 method. Different versions exist for that method: from the simple basic method to more advanced methods such as
22 the quantile perturbation method. In this type of methods, the intrinsic assumption is made that the bias under future
23 climate conditions is identical to the bias in current climate conditions. This is implemented through the use of
24 “change factors” applied for historical precipitation quantiles. Another important assumption that is made by these
25 methods is that the change factors are spatial scale independent, such that the scale difference, although it is an issue
26 for the absolute precipitation intensity values, is less an issue for the delta change methods at which relative changes
27 are applied. The latter assumption is tested next. In this context, the relative changes in precipitation quantiles
28 between the future and historical simulations of climate model runs were calculated to compare the convection-
29 permitting models and their driving GCMs. These change factors were computed for winter and summer seasons as
30 sub-daily and daily precipitation quantiles from the scenario period divided by those from the control period with the
31 same return period (change factor equal to one means no change).

32 The change factors derived from the empirical data, and the ones after use of the extreme value distribution in
33 precipitation extremes for winter and summer seasons computed by the ALARO_{CNRM-CM3} model and the driving
34 CNRM-CM3 GCM are shown in Fig. 7. From a comparison between the empirical data based change factors and
35 those based on the extreme value distributions, it is seen that the extreme value distribution fitting smooths out
36 abrupt changes and random variations in the change factors, making the results easier to interpret. In fact, the

1 distribution fitting removes the randomness involved in the high return periods of the empirical data for summer,
2 leading to a slight difference in the range of changes. However, for the winter season the change factors from the
3 two methods have similar ranges. The change factors obtained from the extreme value distribution fitting are further
4 discussed here. The $ALARO_{CNRM-CM3}$ projects an increasing signal in the range of 26% to 69% for daily winter
5 extremes. The projected increase is even higher for hourly winter extremes, ranging between 37% and 120%. When
6 the change factors computed by the $ALARO_{CNRM-CM3}$ are compared with those obtained from the driving CNRM-
7 CM3 GCM, more or less the same conclusion can be made: an increasing signal for daily winter extremes between
8 23% and 67%. For the summer season, the change factors from the $ALARO_{CNRM-CM3}$ model and the parent CNRM-
9 CM3 GCM are around one, meaning no change in daily summer extremes. However, smaller hourly summer
10 extremes are expected based on the $ALARO_{CNRM-CM3}$ model projections with a decreasing signal down to -26%.
11 Generally, it can be inferred from the results that, at synoptic (daily) scale, the projections by the ALARO model are
12 consistent with those from the driving GCMs. De Troch et al. (2013) pointed out that an increase in spatial
13 resolution in the ALARO model is not as important as the parameterization scheme used for extreme precipitation
14 modeling at the daily scale.

15 Fig. 8 shows the change factors for daily and 3-hourly precipitation computed using the $CCLM_{EC-EARTH}$ model
16 with different spatial resolutions and the driving EC-EARTH GCM for winter and summer seasons. The change
17 factors for all extreme events with $T > 1$ year are shown in this figure. For the winter season, the change factors for
18 both daily and 3-hourly precipitation decrease as the model's resolution increases. Nevertheless, the change factors
19 for all the CCLM runs are higher than those for the driving EC-EARTH GCM. A larger change is projected for 3-
20 hourly precipitation compared with daily precipitation. For summer, the greatest change is obtained for 3-hourly
21 precipitation extremes from the $CCLM_{EC-EARTH}$ 2.8 km run. This increasing signal goes as high as 55%. When the
22 change factors in 3-hourly precipitation extremes from the $CCLM_{EC-EARTH}$ runs are compared with those from the
23 driving EC-EARTH GCM, the results show an amplification of the future climate change signals by the CCLM
24 model: maximum changes of 55%, 11% and 14% respectively for 2.8, 7 and 25 km runs versus a maximum change
25 of 8% for the driving EC-EARTH GCM. This amplification is not evident for the daily scale. Intensification of
26 change in sub-daily precipitation extremes that are not simulated by large scale models was also found by Kendon et
27 al. (2014). The results also reveal that sub-daily precipitation extremes during summer are expected to change at a
28 higher rate compared to daily extremes. Generally, it can be inferred that there is an increase in the change factors of
29 sub-daily precipitation when going from parameterized convection to the convection-permitting scale.

30 **6 Concluding remarks**

31 A comparative study between the convection-permitting climate models with a spatial resolution from 2.8 km up to
32 40 km and driving GCMs or reanalysis data was performed to check whether the models with higher resolution
33 provide more accurate precipitation simulations. Another analysis was performed to validate the spatial scale
34 independency assumption of climate change signals for the delta change downscaling method. The results show that
35 whereas winter daily precipitation extremes are generally overestimated by the ALARO and CCLM models,
36 improved results for summer precipitation extremes are observed especially for sub-daily time scale. This suggests

1 the added value of convection-permitting climate models to simulate summer sub-daily extremes because of either
2 better representation of deep convection or more detail of the land surface. The results moreover indicate that the
3 difference between the convection-permitting models and the parent GCMs or reanalysis data decreases as the time
4 scales get larger (i.e., weekly and monthly). Based on the precipitation statistics derived from IDF curves, the
5 ALARO and CCLM models mostly underestimate local sub-daily precipitation, but still better simulate it compared
6 with parent GCM or reanalysis data when available. Higher precipitation intensities by finer resolution models are a
7 result of better representation of small-scale convective precipitation by these models.

8 To investigate whether or not the climate change signals from the convection-permitting models are more or less
9 the same as those from the large scale driving GCMs, the relative changes were computed for precipitation extremes
10 during summer and winter. For the ALARO model, it can be concluded that, at synoptic (daily) scale, the change
11 factors for the ALARO model are comparable with the ones from the driving CNRM-CM3 GCM. In the case of the
12 CCLM model, the results reveal an intensification of climate change signals for the CCLM model compared with
13 the driving EC-EARTH GCM for the 3-hourly time scale. Comparing change factors for 3-hourly and daily
14 precipitation, a larger change is projected for 3-hourly precipitation for both winter and summer seasons. When the
15 change factors derived from the extreme value distribution are compared with those from the empirical data, it is
16 seen that for both ALARO and CCLM models the climate change signals derived from extreme value distribution
17 fitting are slightly different from the ones obtained from the empirical data for summer due to the removed
18 randomness in the empirical data by the distribution fitting. However, for the winter season the change factors
19 obtained from the two approaches cover more or less the same range.

20 In summary, because the results of this study indicate that the local sub-daily summer precipitation simulations
21 of the high-resolution climate models are closer to the observations, their future projections are expected to be more
22 accurate than those of the driving GCMs. These climate change signals obtained from the high-resolution models
23 may differ from the ones based on the coarse-resolution models, as a result of improved representation of complex
24 landscape and land surface processes in high-resolution models. However, the resulting precipitation change from
25 these high-resolution climate models should not be interpreted as an exact number because of their limited number.
26 More runs with high-resolution models are required to check the consistency among models. In the same way as an
27 ensemble approach on climate models provides uncertainty estimates on the climate change signals, an ensemble of
28 the high-resolution models provides uncertainty estimates on the difference between the climate change signals of
29 fine versus coarse scale. Also, the statistical significance of the difference in climate change signals at fine versus
30 coarse scale can be tested in such approach. From the comparison in this study, the results of the CCLM_{EC-EARTH}
31 model indicate an increase in the change factors in sub-daily summer extremes when going from parameterized
32 convection to the convection-permitting scale. This amplification is not evident at the daily time scale. For the
33 ALARO model also the higher resolution models show changes in the same range as the coarse resolution models
34 for daily precipitation. The differences appear to be a function of time scale, season and climate model. Different
35 procedures for convection parameterization in the CCLM and ALARO models and different boundary conditions
36 (the first one is nested in the EC-EARTH model from CMIP5 and the later in the CNRM-CM3 model from CMIP3)
37 might explain the discrepancy between the results of the two models. The differences in time scale and season is

1 expected to be explained by more realistic simulation of the mesoscale processes involved during sub-daily summer
2 precipitation extremes by convection-permitting models. The results also show an amplification of the change from
3 daily to sub-daily precipitation for both ALARO and CCLM models, which casts a doubt on the validity of the
4 temporal scale independency assumption of climate change signals.

5
6 *Author contributions.* The simulations of the ALARO climate model were performed in the Royal Meteorological
7 Institute of Belgium (RMI) by R. De Troch, O. Giot, R. Hamdi and P. Termonia. The CCLM climate model was
8 implemented by S. Saeed, E. Brisson and N. Van Lipzig in the Earth and Environmental Sciences Department of
9 KU Leuven. H. Tabari and P. Willems developed the methodology and performed the analyses. The paper was
10 prepared by H. Tabari and P. Willems with substantial contributions from all co-authors.

11
12 *Acknowledgements.* This study was partly supported by research projects for the Flemish Environment Agency
13 (Division Operational Water Management and Environmental Reporting), and partly by the Belgian Science Policy
14 Office (CORDEX.be project, BRAIN-be programme) and the European Union's Horizon 2020 research and
15 innovation programme (project BRIGAD, grant agreement No 700699).

16 **References**

- 17 Baldauf, M., Seifert, A., Förstner, J., Majewski, D., Raschendorfer, M., and Reinhardt, T.: Operational convective-
18 scale numerical weather prediction with the COSMO model: Description and sensitivities, *Mon. Weather Rev.*,
19 139(12), 3887–3905, doi:10.1175/MWR-D-10-05013.1, 2011.
- 20 Ban, N., Schmidli, J., and Schar, C.: Evaluation of the convection-resolving regional climate modeling approach in
21 decade-long simulations, *J. Geophys. Res.-Atmos.*, 119, 7889-7907, doi:10.1002/2014JD021478, 2014.
- 22 Ban, N., Schmidli, J., and Schär, C.: Heavy precipitation in a changing climate: Does short-term summer
23 precipitation increase faster?, *Geophys. Res. Lett.*, 42, 1165–1172, doi:10.1002/2014GL062588, 2015.
- 24 Böhm, U., Kücken, M., Ahrens, W., Block, A., Hauße, D., Keuler, K., Rockel, B., and Will, A.: CLM – The
25 Climate Version of LM : Brief Description and Long-Term Applications, *COSMO Newsletters*, 6, 225-235,
26 2006.
- 27 Brisson, E., Demuzere, M., and van Lipzig, N. P. M.: A study on modelling strategies for performing convective
28 permitting climate simulations using the COSMO-CLM over a mid-latitude coastal region, *Meteor. Z.*, doi:
29 10.1127/metz/2015/0598, 2015.
- 30 Brisson, E., Van Weverberg, K., Demuzere, M., Devis, A., Saeed, S., Stengel, M., and van Lipzig, N. P. M.: How
31 well can a convection-permitting climate model reproduce decadal statistics of precipitation, temperature and
32 cloud characteristics?, *Climate Dynam.*, doi: 10.1007/s00382-016-3012-z, 2016.
- 33 Chan, S. C., Kendon, E. J., Fowler, H. J., Blenkinsop, S., Ferro, C. A. T., and Stephenson, D. B.: Does increasing
34 the spatial resolution of a regional climate model improve the simulated daily precipitation?, *Climate Dynam.*,
35 41, 1475–1495, doi: 10.1007/s00382-012-1568-9, 2013.

1 Chan, S. C., Kendon, E. J., Fowler, H. J., Blenkinsop, S., Roberts, N. M., and Ferro, C. A.: The value of high-
2 resolution met office regional climate models in the simulation of multi-hourly precipitation extremes, *J. Clim.*,
3 27(16), 6155–6174, doi:10.1175/JCLI-D-13-00723.1, 2014.

4 Christensen, J. H., and Christensen, O. B.: A summary of the PRUDENCE model projections of changes in
5 European climate by the end of this century, *Climatic Change* 81, 7–30, doi:10.1007/s10584-006-9210-7, 2007.

6 De Troch, R., Hamdi, R., Van De Vyver, H., Geleyn, J.-F., and Termonia, P.: Multiscale performance of the
7 ALARO-0 model for simulating extreme summer precipitation climatology in Belgium, *J. Climate*, 26, 8895-
8 8915, doi:10.1175/JCLI-D-12-00844.1, 2013.

9 Demarée, G. R.: Le pluviographe centenaire du plateau d’Uccle: son histoire, ses données et ses applications, *La*
10 *Houille Blanche*, 4, 95–102, doi:10.1051/lhb/2003082, 2003.

11 Deng, H., Luo, Y., Yao, Y., and Liu, C.: Spring and summer precipitation changes from 1880 to 2011 and the future
12 projections from CMIP5 models in the Yangtze River Basin, China, *Quatern. Int.*, 304, 95–106,
13 doi:10.1016/j.quaint.2013.03.036, 2013.

14 Done, J., Davis, C. A., and Weisman, M.: The next generation of NWP: Explicit forecasts of convection using the
15 Weather Research And Forecasting (WRF) model, *Atmos. Sci. Lett.*, 5(6), 110–117, doi: 10.1002/asl.72, 2004.

16 Fossier, G.: Precipitation statistics from regional climate model at resolutions relevant for soil erosion, KIT Scientific
17 Publishing, Karlsruhe, 2014.

18 Fossier, G., Khodayar, S., and Berg, P.: Benefit of convection permitting climate model simulations in the
19 representation of convective precipitation, *Climate Dynam.*, 44, 45-60, doi:10.1007/s00382-014-2242-1, 2015.

20 Fossier, G., Khodayar, S., and Berg, P.: Climate change in the next 30 years: What can a convection-permitting
21 model tell us that we did not already know?, *Climate Dynam.*, doi: 10.1007/s00382-016-3186-4, 2016.

22 Gudmundsson, L., Bremnes, J. B., Haugen, J. E., and Engen-Skaugen, T.: Downscaling RCM precipitation to the
23 station scale using statistical transformations – a comparison of methods, *Hydrol. Earth Syst. Sc.*, 16, 3383–
24 3390, doi:10.5194/hess-16-3383-2012, 2012.

25 Hamdi, R., Van de Vyver, H., De Troch, R., and Termonia, P.: Assessment of three dynamical urban climate
26 downscaling methods: Brussels’s future urban heat island under an A1B emission scenario, *Int. J. Climatol.*, 34,
27 978–999, doi:10.1002/joc.3734, 2014.

28 Haylock, M. R., Hofstra, N., Klein Tank, A. M. G., Klok, E. J., Jones, P. D., and New, M.: A European daily high-
29 resolution gridded dataset of surface temperature and precipitation, *J. Geophys. Res (Atmospheres)*, 113,
30 D20119, doi:10.1029/2008JD10201, 2008.

31 Hofstra, N., Haylock, M., New, M., and Jones, P. D.: Testing EOBS European high-resolution gridded data set of
32 daily precipitation and surface temperature, *J. Geophys. Res.*, 144, D21101, doi:10.1029/2009JD011799, 2009.

33 Hohenegger, C., Brockhaus, P., and Schar, C.: Towards climate simulations at cloud-resolving scales, *Meteor. Z.*,
34 17, 383–394, doi:10.1127/0941-2948/2008/0303, 2008.

35 Hong, S. Y., and Leetmaa, A.: An evaluation of the NCEP RSM for regional climate modeling, *J. Climate*, 12, 592–
36 609, doi:10.1175/1520-0442(1999)012<0592:AEOTNR>2.0.CO;2, 1999.

1 Ikeda, K., et al.: Simulation of seasonal snowfall over Colorado, *Atmos. Res.*, 97(4), 462–477,
2 doi:10.1016/j.atmosres.2010.04.010, 2010.

3 IPCC: IPCC Fourth Assessment Report (AR4), Cambridge University Press, Cambridge, 2007.

4 IPCC: The Scientific Basis. Contribution of Working Group I to the Third Assessment Report of the
5 Intergovernmental Panel on Climate Change [Houghton, J.T., et al. (eds.)], Cambridge University Press,
6 Cambridge, United Kingdom and New York, NY, USA, 881 p, 2001.

7 IPCC: Summary for Policymakers. Climate Change 2013: The Physical Science Basis, Contribution of Working
8 Group I to the Fifth Assessment Report of the Intergovernmental Panel on Climate Change, In: Stocker, T. F.,
9 Qin, D., Plattner, G.-K., Tignor, M., Allen, S. K., Boschung, J., Nauels, A., Xia, Y., Bex, V., and Midgley, P. M.
10 (Eds.), 2013.

11 Jacob, D., et al.: EURO-CORDEX: new high-resolution climate change projections for European impact research,
12 *Reg. Environ. Change*, 14, 563–578, doi:10.1007/s10113-013-0499-2, 2014.

13 Johnson, F., Westra, S., Sharma, A., and Pitman, A. J.: An assessment of GCM skill in simulating persistence across
14 multiple time scales, *J. Climate*, 24(14), 3609–3623, doi: 10.1175/2011JCLI3732.1, 2011.

15 Kendon, E. J., Roberts, N. M., Fowler, H. J., Roberts, M. J., Chan, S. C., and Senior, C. A.: Heavier summer
16 downpours with climate change revealed by weather forecast resolution model, *Nature Climate Change*, 4, 570–
17 576, doi:10.1038/nclimate2258, 2014.

18 Kendon, E. J., Roberts, N. M., Senior, C. A., and Roberts, M. J.: Realism of rainfall in a very high-resolution
19 regional climate model, *J. Climate*, 25, 5791–5806, doi: 10.1175/JCLI-D-11-00562.1, 2012.

20 Maraun, D.: Bias correction, quantile mapping, and downscaling: revisiting the inflation issue, *J. Climate*, 26: 2137–
21 2143, doi:10.1175/JCLI-D-12-00821.1, 2013.

22 Maraun, D., et al.: Precipitation downscaling under climate change: Recent developments to bridge the gap between
23 dynamical models and the end user, *Rev. Geophys.*, 48, RG3003, doi:10.1029/2009RG000314, 2010.

24 Masson, D., and Knutti, R.: Spatial-scale dependence of climate model performance in the CMIP3 ensemble, *J.*
25 *Climate*, 24, 2680–2692, doi: <http://dx.doi.org/10.1175/2011JCLI3513.1>, 2011.

26 Mayer, S., et al.: Identifying added value in high-resolution climate simulations over Scandinavia, *Tellus A.*, 67,
27 doi:<http://dx.doi.org/10.3402/tellusa.v67.24941>, 2015.

28 Mearns, L. O., Giorgi, F., Whetton, P., Pabon, D., Hulme, M., and Lal, M.: Guidelines for use of climate scenarios
29 developed from regional climate model experiments. Data Distribution Centre of the Intergovernmental Panel on
30 Climate Change, 2004.

31 Mearns, L. O., et al.: Climate change projections of the North American Regional Climate Change Assessment
32 Program (NARCCAP), *Climatic Change*, 120, 965–975, doi:10.1007/s10584-013-0831-3, 2013.

33 Ntegeka, C., Baguis, P., Roulin, E., and Willems, P.: Developing tailored climate change scenarios for hydrological
34 impact assessments, *J. Hydrol.*, 508, 307–321, doi:10.1016/j.jhydrol.2013.11.001, 2014.

35 Olsson, J., Willén, U., and Kawamura, A.: Downscaling extreme short-term regional climate model precipitation for
36 urban hydrological applications, *Hydrol. Res.*, 43, 341–351, doi:10.2166/nh.2012.135, 2012.

1 Olsson, J., Berg, P., and Kawamura, A.: Impact of RCM spatial resolution on the reproduction of local, subdaily
2 precipitation, *J. Hydrometeorol.*, 16(2), 534-547, doi:10.1175/JHM-D-14-0007.1, 2015.

3 Prein, A. F., Gobiet, A., Suklitsch, M., Truhetz, H., Awan, N. K., Keuler, K., and Georgievski, G.: Added value of
4 convection permitting seasonal simulations, *Climate Dynam.*, 41, 2655-2677, doi:10.1007/s00382-013-1744-6,
5 2013a.

6 Prein, A., Holland, G. A., Rasmussen, R. M., Done, J., Ikeda, K., Clark, M. P., and Liu, C. H.: Importance of
7 Regional Climate Model Grid Spacing for the Simulation of Heavy Precipitation in the Colorado Headwaters, *J.*
8 *Climate*, 26, 4848–4857, doi:10.1175/JCLI-D-12-00727.1, 2013b.

9 Prein, A.F., et al.: A review on regional convection-permitting climate modeling: demonstrations, prospects, and
10 challenges, *Rev. Geophys.*, doi: 10.1002/2014RG000475, 2015.

11 Rajczak, J., Pall, P., and Schär, C.: Projections of extreme precipitation events in regional climate simulations for
12 Europe and the Alpine Region, *J. Geophys. Res.-Atmos.*, 118, 3610–3626, doi:10.1002/jgrd.50297, 2013.

13 Rana, A., Foster, K., Bosshard, T., Olsson, J., and Bengtsson, L.: Impact of climate change on rainfall over
14 Mumbai using Distribution-based Scaling of Global Climate Model projections, *J. Hydrol. Reg. Stud.*, 1, 107–
15 128, doi:10.1016/j.ejrh.2014.06.005, 2014.

16 Rasmussen, R., et al.: High-resolution coupled climate runoff simulations of seasonal snowfall over Colorado: A
17 process study of current and warmer climate, *J. Clim.*, 24(12), 3015–3048, 2011.

18 Rauscher, S. A., Coppola, E., Piani, C., and Giorgi, F.: Resolution effects on regional climate model simulations of
19 seasonal precipitation over Europe, *Climate Dynam.*, 35, 685–711, doi: 10.1007/s00382-009-0607-7, 2010.

20 Rockel, B., Will, A., and Hense, A.: The Regional Climate Model COSMO-CLM (CCLM), *Meteor. Z.*, 17, 347–
21 348, doi:10.1127/0941-2948/2008/0309, 2008.

22 Steppeler, J., Doms, G., Schättler, U., Bitzer, H. W., Gassmann, A., Damrath, U., and Gregoric, G.: Meso-gamma
23 scale forecasts using the nonhydrostatic model LM, *Meteor. Atmos. Phys.*, 82, 75-96, doi:10.1007/s00703-001-
24 0592-9, 2003.

25 Sun, Q., Miao, C., and Duan, Q.: Projected changes in temperature and precipitation in ten river basins over China in
26 21st century, *Int. J. Climatol.*, 35, 1125–1141, doi: 10.1002/joc.4043, 2015.

27 Sunyer, M. A., et al.: Inter-comparison of statistical downscaling methods for projection of extreme precipitation in
28 Europe, *Hydrol. Earth Syst. Sc.* 19, 1827-1847, doi:10.5194/hess-19-1827-2015, 2015.

29 Sunyer, M.A., Sørup, H.J.D., Christensen, O.B., Madsen, H., Rosbjerg, D., Mikkelsen, P.S., and Arnbjerg-Nielsen,
30 K.: On the importance of observational data properties when assessing regional climate model performance of
31 extreme precipitation. *Hydrology and Earth System Sciences*, 17(11), 4323-4337, doi:10.5194/hess-17-4323-
32 2013, 2013.

33 Tabari, H., AghaKouchak, A., and Willems, P.: A perturbation approach for assessing trends in precipitation
34 extremes across Iran, *J. Hydrol.*, 519, 1420–1427, doi:10.1016/j.jhydrol.2014.09.019, 2014.

35 Tabari, H., and Willems, P.: Daily precipitation extremes in Iran: decadal anomalies and possible drivers, *J. Am.*
36 *Water Resour. As.*, 52: 541–559, doi:10.1111/1752-1688.12403, 2016.

- 1 Tabari, H., Taye, M.T., and Willems, P.: Water availability change in central Belgium for the late 21st century,
2 Global Planet. Change, 131: 115–123, doi:10.1016/j.gloplacha.2015.05.012, 2015.
- 3 Tang, Y., Lean, H. W., and Bornemann, J.: The benefits of the met office variable resolution NWP model for
4 forecasting convection, Meteorol. Appl., 20(4), 417–426, doi:10.1002/met.1300, 2013.
- 5 van Haren, R., van Oldenborgh, G. J., Lenderink, G., and Hazeleger, W.: Evaluation of modeled changes in extreme
6 precipitation in Europe and the Rhine basin, Environ. Res. Lett., 8, 014053, doi:10.1088/1748-9326/8/1/014053,
7 2013.
- 8 van Pelt, S. C., Beersma, J. J., Buishand, T. A., van den Hurk, B. J. J. M., and Kabat P.: Future changes in extreme
9 precipitation in the Rhine basin based on global and regional climate model simulations, Hydrol. Earth Syst. Sci.,
10 16, 4517–4530, doi: 10.5194/hess-16-4517-2012, 2012.
- 11 Willems, P.: Compound IDF-relationships of extreme precipitation for two seasons and two storm types, J. Hydrol.,
12 233: 189–205, doi:10.1016/S0022-1694(00)00233-X, 2000.
- 13 Willems, P.: A time series tool to support the multi-criteria performance evaluation of rainfall-runoff models,
14 Environ. Modell. Softw., 24: 311–321, doi:10.1016/j.envsoft.2008.09.005, 2009.
- 15 Willems, P.: Revision of urban drainage design rules after assessment of climate change impacts on precipitation
16 extremes at Uccle, Belgium, J. Hydrol., 496, doi:10.1016/j.jhydrol.2013.05.037, 166–177, 2013.
- 17 Willems, P., Arnbjerg-Nielsen, K., Olsson, J., and Nguyen, V.-T.-V.: Climate change impact assessment on urban
18 rainfall extremes and urban drainage: Methods and shortcomings, Atmos. Res., 103, 106–118,
19 doi:10.1016/j.atmosres.2011.04.003, 2012.
- 20 Willems, P., and Vrac, M.: Statistical precipitation downscaling for small-scale hydrological impact investigations
21 of climate change, J. Hydrol., 402, 193–205, doi:10.1016/j.jhydrol.2011.02.030, 2011.

Table 1 The convection-permitting model runs used in this study.

Climate model	Driving GCM/reanalysis	Spatial scale (km)	Temporal scale	Control period	Scenario period	Data coverage
CCLM	ERA-Interim	2.8	15 min	2001-2010	-	whole year
	ERA-Interim	7	hourly	2001-2010	-	whole year
	ERA-Interim	25	3 hourly	2001-2010	-	whole year
	EC-EARTH	2.8	15 min ¹	2001-2010	2060-2069	whole year
	EC-EARTH	7	hourly	2001-2010	2060-2069	whole year
	EC-EARTH	25	3 hourly	2001-2010	2060-2069	whole year
ALARO	ERA-Interim	4	hourly	1981-2010	-	whole year
	CNRM-CM3	4	hourly	1961-1990	2071-2100	whole year
	ERA40	4	hourly	1961-1990	-	summer
	ERA40	10	hourly	1961-1990	-	summer
	ERA40	40	hourly	1961-1990	-	summer

¹ CCLM_{EC-EARTH} data for the scenario period are available for the hourly time scale.

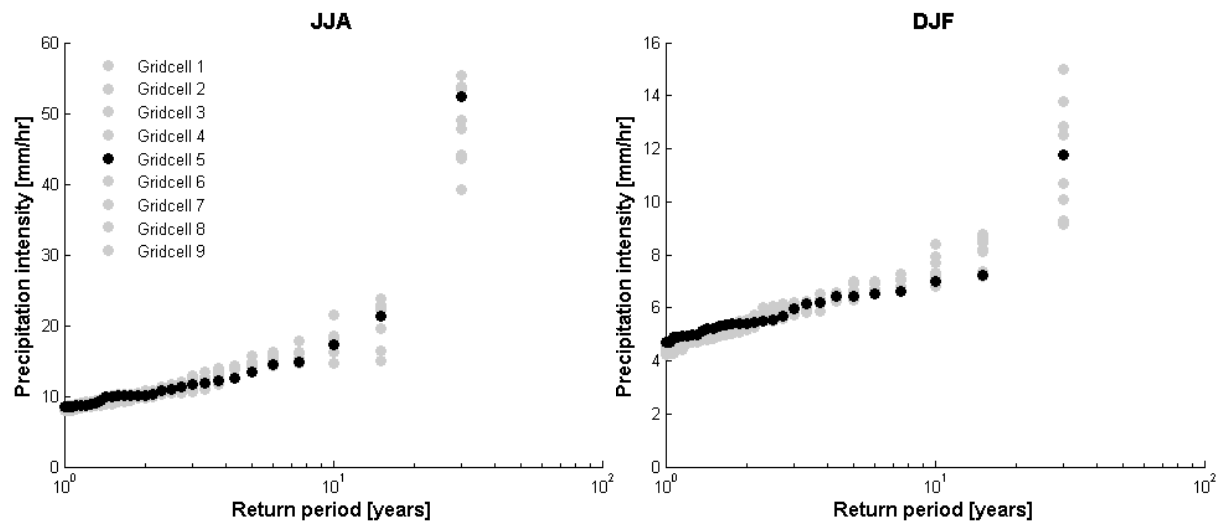


Figure 1. Hourly precipitation extremes in a matrix of 3×3 ALARO_{ERA-Interim} 4 km model grid points surrounding the closest model grid point to Uccle (Gridcell 5), for summer (left) and winter (right) seasons (historical climate: 1961-1990).

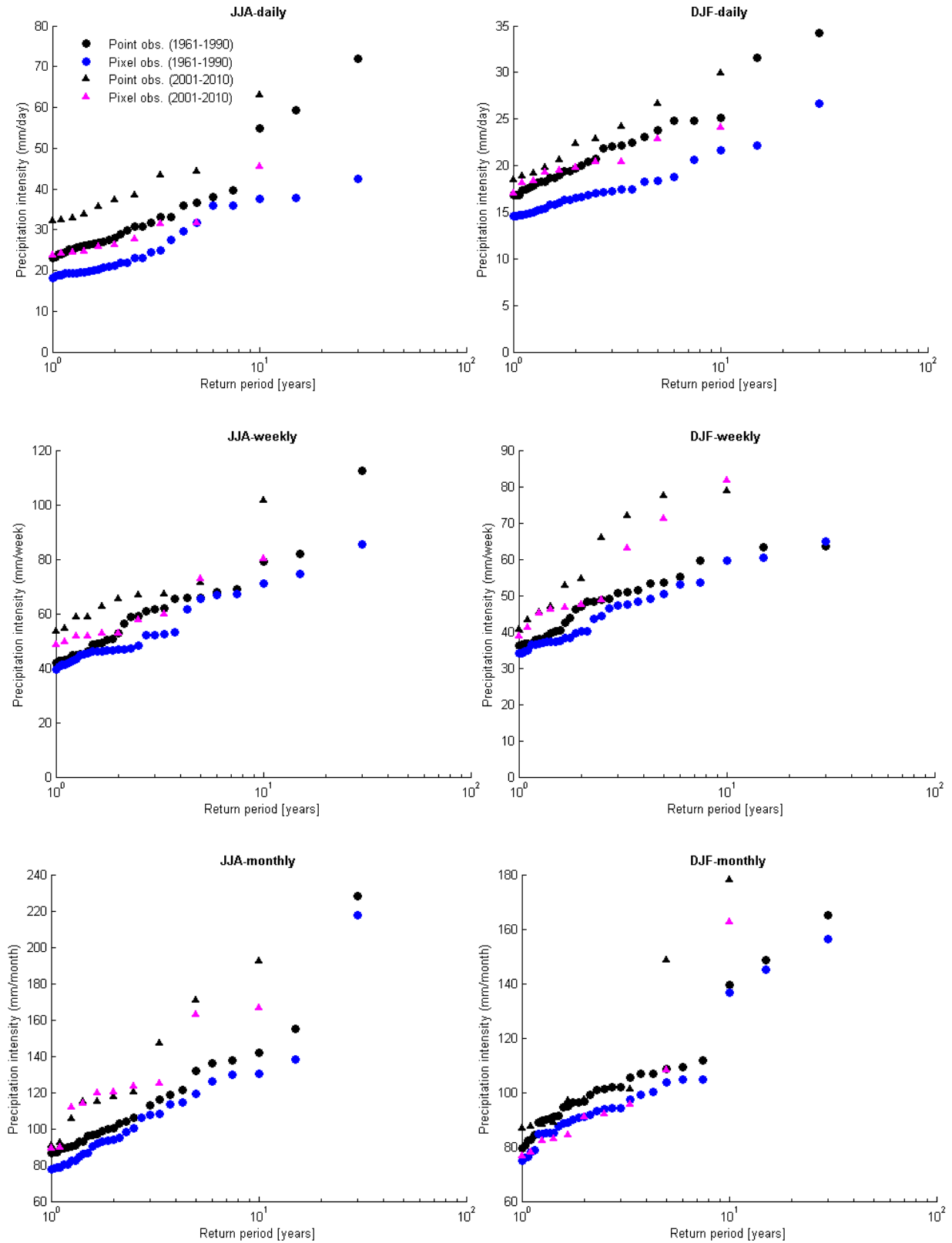


Figure 2. Comparison between point and pixel interpolated (spatial resolution of 27.8 km) Uccle precipitation of different time scales for summer (left column) and winter (right column).

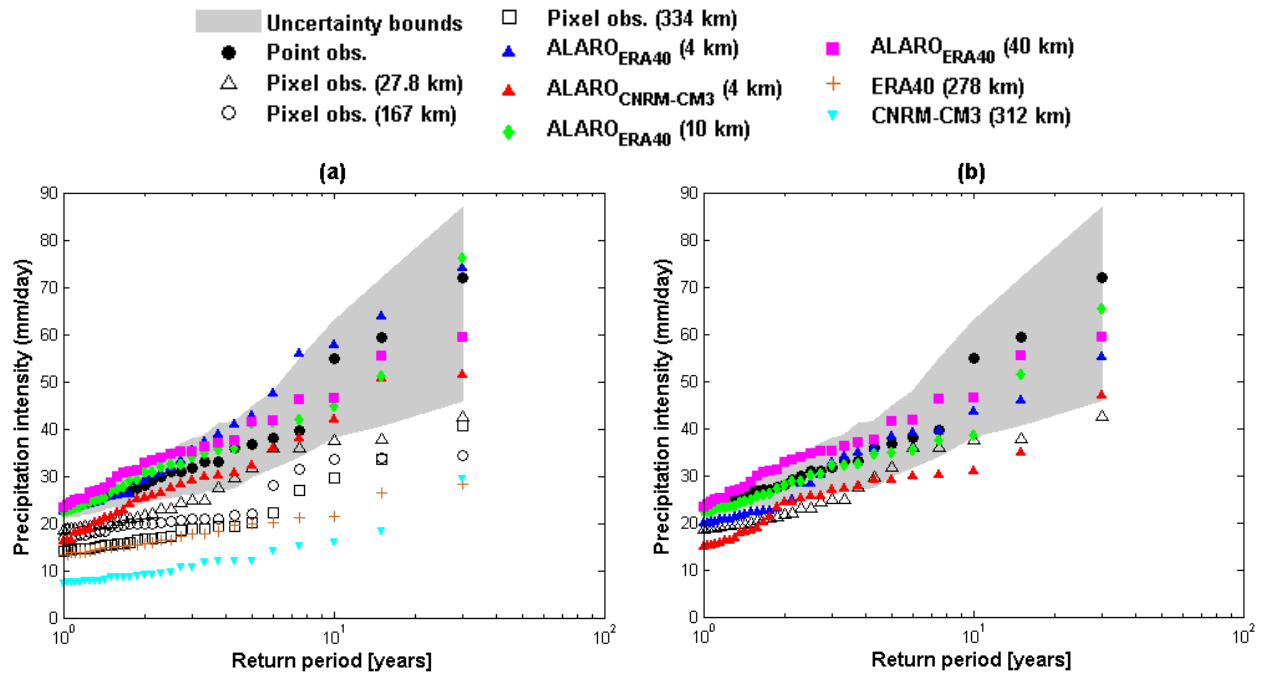


Figure 3. Validation of the native (a) and aggregated (b) daily precipitation quantiles (1961-1990) for the ALARO model and its driving GCM or reanalysis data based on Uccle observations, for summer season (shaded areas show at-site confidence intervals for the point observations using the bootstrap-based 95% confidence intervals).

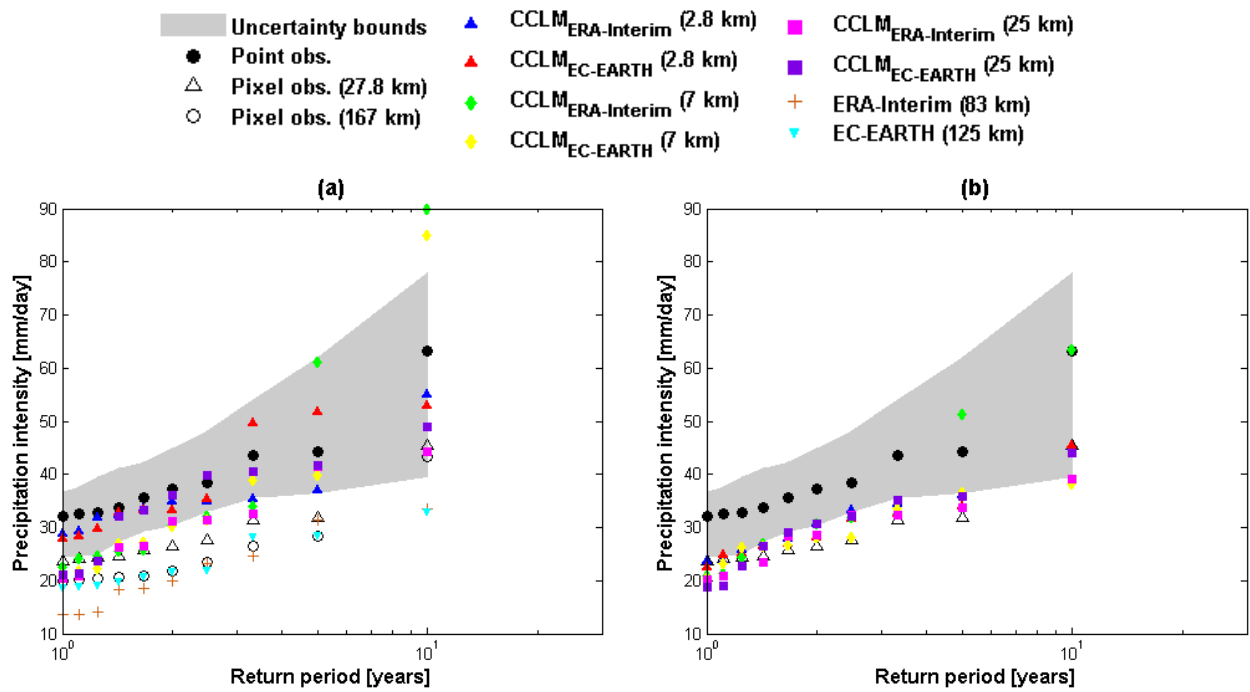


Figure 4. Validation of the native (a) and aggregated (b) daily precipitation quantiles (2001-2010) for the CCLM model and its driving GCM or reanalysis data based on Uccle observations, for summer season (shaded areas show at-site confidence intervals for the point observations using the bootstrap-based 95% confidence intervals).

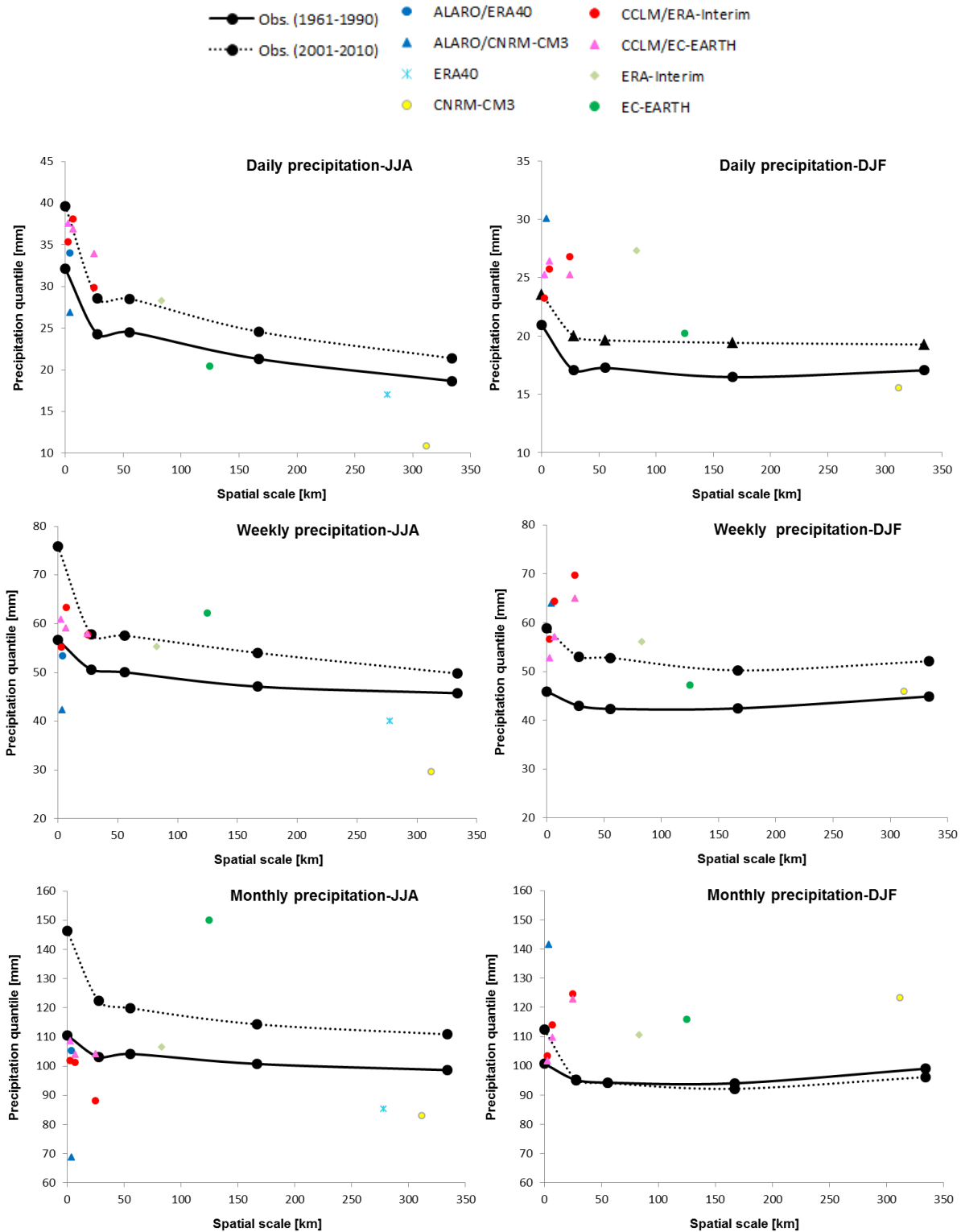


Figure 5. Validation of the extreme precipitation (averaged over the extreme events with $T > 1$ year) simulations for the ALARO, CCLM and the driving GCMs or reanalysis data based on point and pixel interpolated Uccle observations for summer (left) and winter (right) seasons, versus the models' spatial scale.

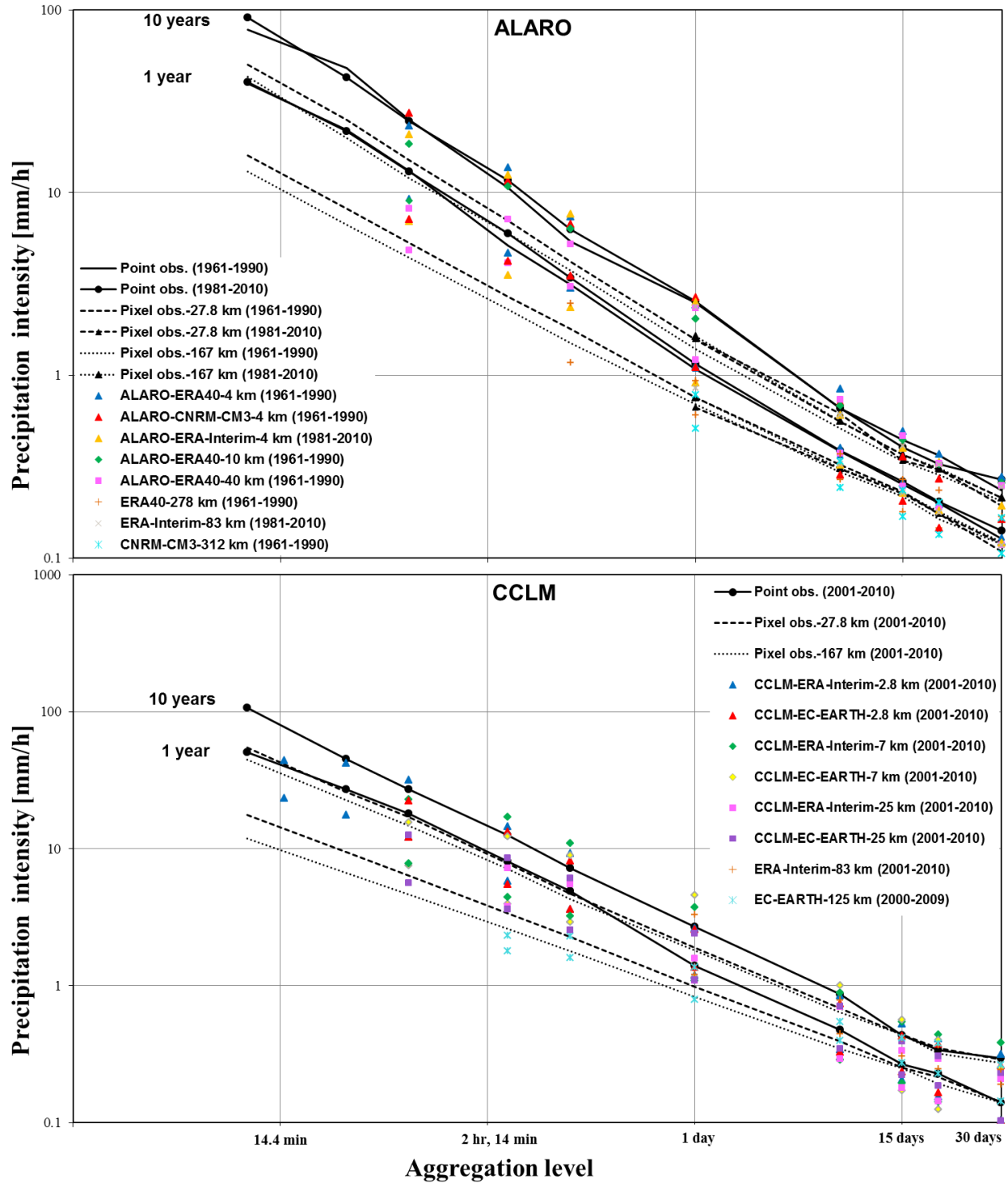


Figure 6. Comparison of historical IDF-relationships based on point and pixel interpolated Uccle observations, with the CCLM, ALARO and the driving GCM or reanalysis results for summer season (IDF curves for the E-OBS pixel data were extrapolated for the sub-daily time scales based on extreme value distribution).

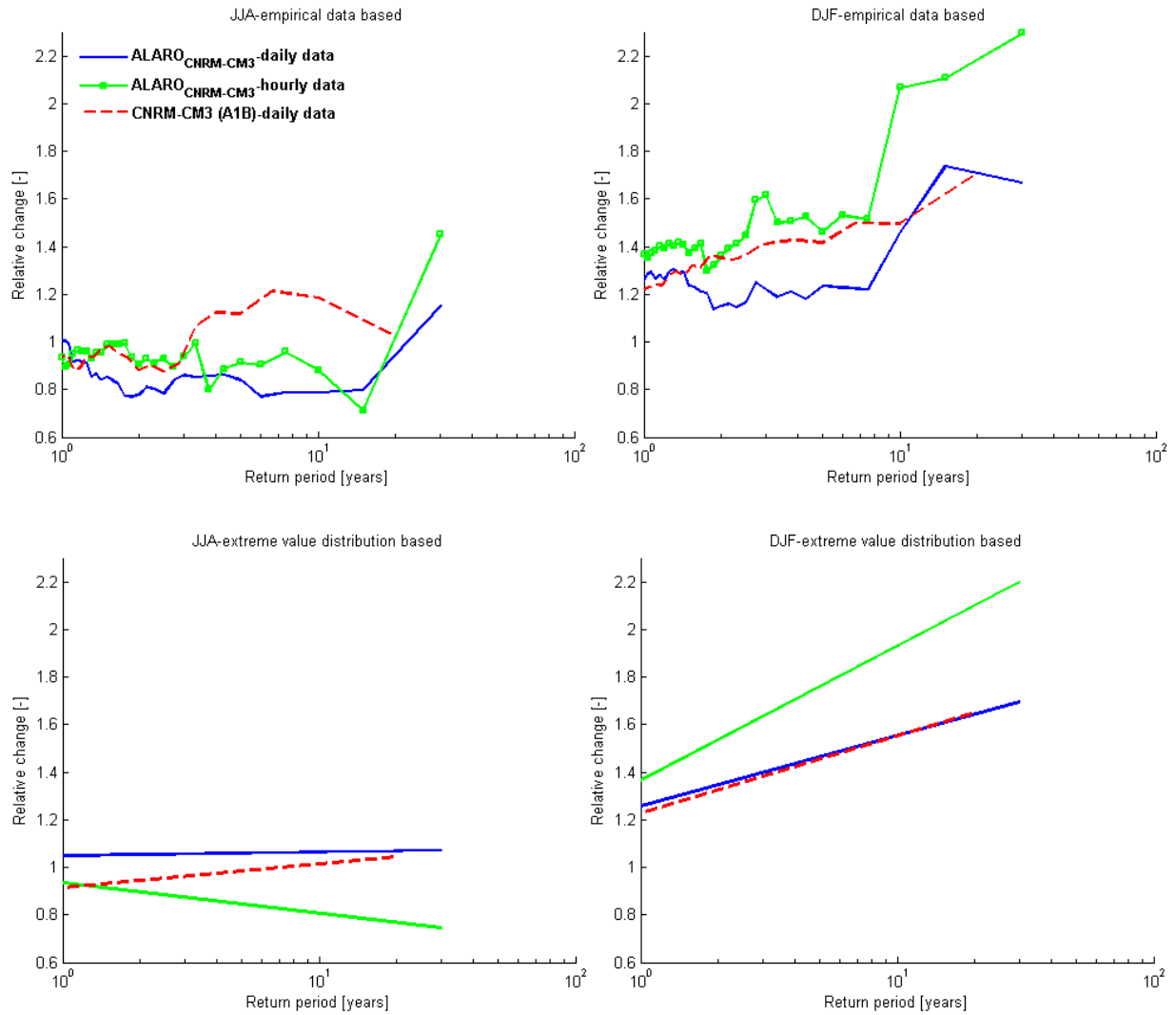


Figure 7. Change factors for daily and hourly precipitation quantiles computed using the ALARO_{CNRM-CM3} 4 km and the driving CNRM-CM3 (A1B) for summer (left column) and winter (right column) seasons, obtained from the empirical data (top figures) and after use of the extreme value distributions (bottom figures).

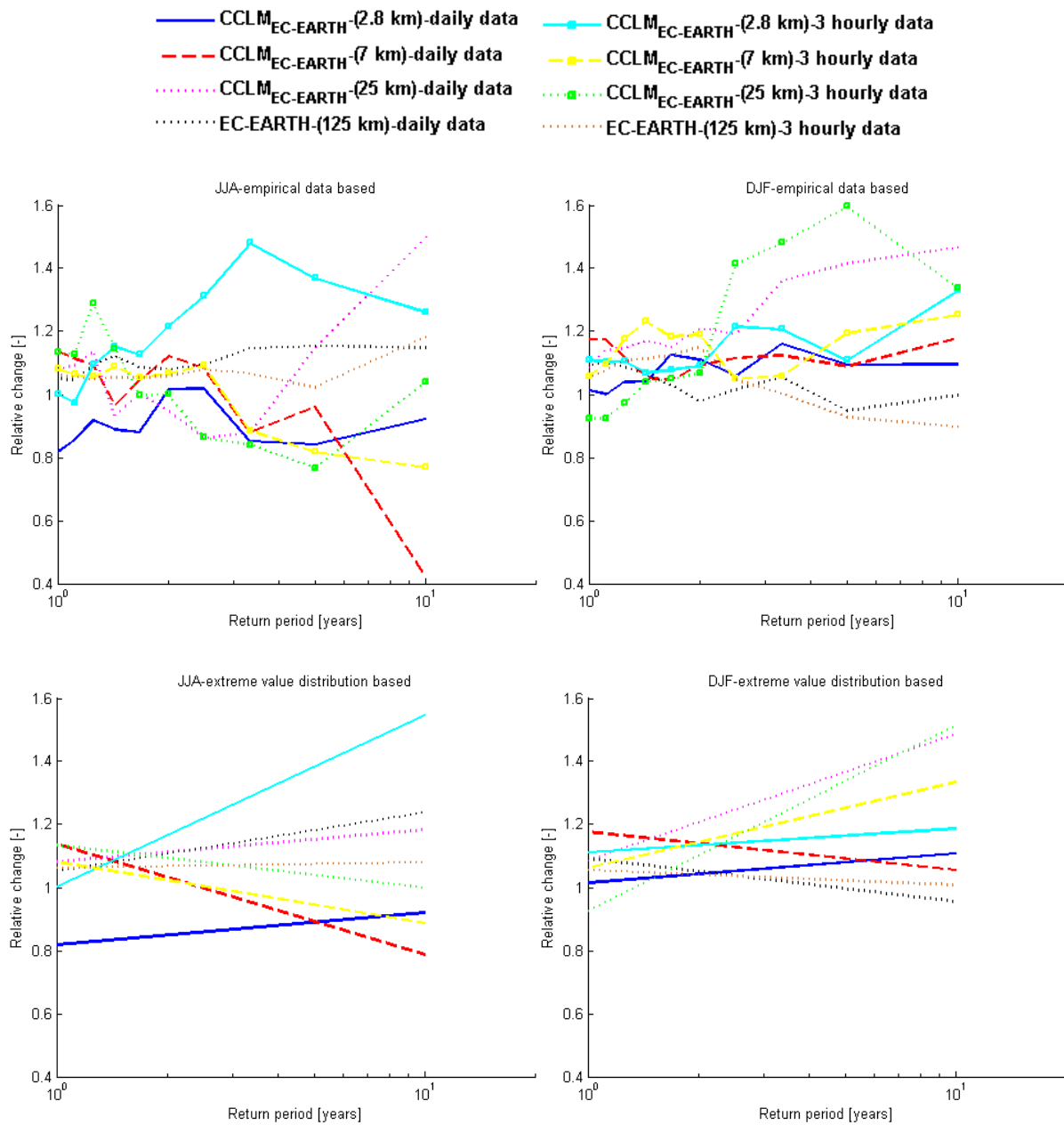


Figure 8. Change factors for daily and 3-hourly precipitation quantiles computed using the CCLM_{EC-EARTH} 2.8, 7, 25 km for summer (left column) and winter (right column) seasons, obtained from the empirical data (top figures) and after use of the extreme value distributions (bottom figures).